Slaughter, C. A., Jeske, D. J., Kuziel, W. A., Milner, C. B., & Capra, J. D. (1984) *J. Immunol. 132*, 3164.
Smith, J. A., & Margolies, M. N. (1984) *Biochemistry 23*, 4726.
Spiess, J., Rivier, J., & Vale, W. (1983) *Biochemistry 22*, 4341.
Steiner, L. A., Garcia-Pardo, A., & Margolies, M. N. (1979) *Biochemistry 18*, 4068.
Wysocki, L., & Sato, V. (1981) *Eur. J. Immunol. 11*, 832.
Wysocki, L. J., Margolies, M. N., Huang, B., Nemazee, D. A., Wechsler, D. S., Sato, V. L., Smith, J. A., & Gefter, M. L. (1985) *J. Immunol. 134*, 2740.

Kinetic Analysis of Guanosine 5′-*O*-(3-Thiotriphosphate) Effects on Phosphatidylinositol Turnover in NRK Cell Homogenates†

Suresh B. Chahwala,‡,§ Laurie F. Fleischman,‖ and Lewis Cantley*,‡
Department of Physiology, Tufts University School of Medicine, Boston, Massachusetts 02111, and Department of Cellular and Developmental Biology, Harvard University, Cambridge, Massachusetts 02138
Received July 22, 1986; Revised Manuscript Received September 24, 1986

ABSTRACT: Addition of the guanine nucleotide analogue guanosine 5′-*O*-(3-thiotriphosphate) (GTPγS) to [^{3}H]inositol-labeled NRK cell homogenates resulted in rapid breakdown of cellular polyphosphoinositides. GTPγS stimulated phospholipase C, resulting in a more than 4-fold increase in the hydrolysis rates of phosphatidylinositol 4-phosphate (PIP) and phosphatidylinositol 4,5-bis(phosphate) (PIP_2). No significant effect of GTPγS on direct phosphatidylinositol (PI) hydrolysis was detected. There was an increase in water-soluble inositols, with inositol tris(phosphate) (IP_3) levels increasing at least 10 times over the decrease seen in PIP_2, indicating that PIP kinase activity was also accelerated following GTPγS addition. Inositol 1,4,5-tris(phosphate) peaked rapidly after GTPγS addition (less than 2 min) while inositol 1,3,4-tris(phosphate) was produced more slowly and leveled off after approximately 10 min. The differential equations describing conversion between intermediates in the PI turnover pathway were solved and fitted to data obtained from both [^{3}H]inositol and [^{32}P]phosphate fluxes by nonlinear least-squares analysis. GTPγS effects on the pseudo-first-order rate constants for the lipase, kinase, and phosphatase steps were determined from the analysis. From these measurements it can be estimated that, in the presence of GTPγS and calcium buffered to 130 nM, hydrolysis of PIP_2 accounts for at least 10 times as much diacylglycerol as direct PI breakdown despite the 100-fold excess of PI over PIP_2. From the kinetic model it is predicted that small changes in the activities of PI and PIP kinases can have large but different effects on the level of IP_3 and diacylglycerol following GTPγS addition. These results argue that regulation of PI and PIP kinases may be important for determining both cellular IP_3 and diacylglycerol levels.

Stimulation of cells by a variety of hormones and mitogens activates a transducing mechanism that involves phosphoinositide breakdown (Berridge & Irvine, 1984; Macara, 1985; Whitman et al., 1986a). The key reaction of this transducing mechanism is a receptor-mediated hydrolysis of phosphatidylinositol 4,5-bis(phosphate) (PIP_2)[1] to give diacylglycerol (DG) and inositol tris(phosphate) (IP_3) (Berridge, 1984). IP_3 and DG have both been shown to act as second messengers, IP_3 by mobilizing intracellular Ca^{2+} (Streb et al., 1983) and DG by stimulating protein kinase C (Nishizuka, 1984). Although much of the study of PI turnover has been in terminally differentiated and nonproliferating cells that show responses to specific hormones, it has been argued that this system originally evolved for regulation of cell growth and was later adapted for specific tissue responses (Macara, 1985; Whitman et al., 1986a). A role for PI turnover in normal cell proliferation has been suggested by the ability of Ca^{2+} ionophore A23187 and specific activators of protein kinase C such as phorbol esters to mimic or enhance early effects of growth factors on quiescent cells (Mastro & Smith, 1983). Tumorigenesis is associated with the uncontrolled proliferation of cells, and specific oncogenes have been implicated in this process (Bishop, 1985). Cells transformed by several types of oncogenes have accelerated PI turnover compared with nontransformed cells, suggesting that enhanced PI turnover may be a critical part of the transformation mechanism (Diringer & Friis, 1977; Sugimoto et al., 1984; Macara et al., 1984; Fleischman et al., 1986; Kaplan et al., 1986).

The mechanism by which hormones, mitogens, and certain oncogene products activate PI turnover is unknown. The lack

† This work was supported by National Institutes of Health Grants GM 36133 and GM 36624. L.C. is an Established Investigator of the American Heart Association.
* Address correspondence to this author.
‡ Tufts University School of Medicine.
§ Present address: Pfizer Ltd., Discovery Biology, Sandwich, Kent, DT13 9NJ, U.K.
‖ Harvard University.

[1] Abbreviations: PI, phosphatidylinositol; PIP, phosphatidylinositol 4-phosphate; PIP_2, phosphatidylinositol 4,5-bis(phosphate); IP_1, inositol 1-phosphate; IP_2, inositol 1,4-bis(phosphate); IP_3, inositol 1,4,5-tris(phosphate) + inositol 1,3,4-tris(phosphate); Ins-1,4,5-P_3 or IP_3(1,4,5), inositol 1,4,5-tris(phosphate); Ins-1,3,4-P_3 or IP_3(1,3,4), inositol 1,3,4-tris(phosphate); Ins-1,3,4,5-P_4 or IP_4(1,3,4,5), inositol 1,3,4,5-tetrakis(phosphate); ADP, adenosine 5′-diphosphate; ATP, adenosine 5′-triphosphate; GDP, guanosine 5′-diphosphate; GTP, guanosine 5′-triphosphate; GTPγS, guanosine 5′-*O*-(3-thiotriphosphate); DG, diacylglycerol; Hepes, 4-(2-hydroxyethyl)-1-piperazineethanesulfonic acid; EGTA, ethylene glycol bis(β-aminoethyl ether)-*N*,*N*,*N*′,*N*′-tetraacetic acid; TLC, thin-layer chromatography; HPLC, high-performance liquid chromatography.

0006-2960/87/0426-0612$01.50/0 © 1987 American Chemical Society

of understanding of these pathways is a result of the difficulty in demonstrating hormone, mitogen, or oncogene activation of PI turnover in subcellular systems. The observation that a subclass of cellular PI and PIP kinases specifically bind to the complex of middle t/pp60$^{c\text{-}src}$ in cells transformed by the polyoma middle t gene product suggests that these enzymes may be activated by this oncogene (Kaplan et al., 1986; Whitman et al., 1986b). However, it has not yet been possible to determine whether these enzymes are regulated by this association. The recent observation that GTP or the GTP analogue GTPγS can activate PI turnover in lysed or permeabilized cells from a variety of tissues has suggested that a GTP binding protein mediates the response to certain hormones (Cantau et al., 1980; Moreno et al., 1983; Masters et al., 1985). The GTP binding protein(s) that mediates (mediate) these responses has (have) not been identified. In any event, the ability of GTP to stimulate PI turnover has provided a subcellular system that can be better controlled than the intact cell and should allow a better understanding of the mechanism by which this complex pathway is regulated. The effect of GTP on proliferating cells in which PI turnover is controlled by growth factors has not been investigated.

As a first step toward our ultimate goal of understanding regulation of PI turnover by oncogenes and growth factors, we have investigated the effect of GTPγS on PI turnover in both homogenized and permeabilized NRK fibroblasts. These cells were chosen for the study since we have previously characterized the steady-state levels of intermediates in the PI pathway in both transformed and normal counterparts and have investigated growth factor stimulation of the pathway (Fleischman et al., 1986; Chahwala & Cantley, 1986). Seven intermediates in the pathway (PI, PIP, PIP_2, Ins-1,4,5-P_3, Ins-1,3,4-P_3, IP_2, and IP) were monitored in parallel by using label in the inositol moiety, and the results were compared with fluxes by using [^{32}P]phosphate label. We present kinetic evidence that GTPγS stimulates breakdown of both PIP_2 and PIP at concentrations of Ca^{2+} pertaining in resting cells. We also show that conversion of PI to PIP and PIP_2 is enhanced during GTPγS-induced hydrolysis of phosphoinositides. The kinetic equations used to determine the rate constants predict that small changes in PI and PIP kinases can have significant effects on GTPγS-stimulated production of IP_3 and diacylglycerol. A theoretical framework for evaluating inositol and phosphate fluxes in more complex whole cell systems is provided by the equations in the Appendix.

Materials and Methods

Materials. MgATP was obtained from Sigma. [^{32}P]-Orthophosphoric acid and [2-^{3}H]-*myo*-inositol were from New England Nuclear. [γ-^{32}P]ATP was synthesized with carrier-free $^{32}PO_4^{3-}$ and Gamma Prep A (Promega). GTPγS and Dowex A8 resin were from Boehringer Mannheim and Fluka, respectively. All other chemicals were of reagent grade.

Cell Cultures. NRK cells were a generous gift from Dr. R. J. Goldberg of Merck Sharp & Dohme. NRK cells were grown in Dulbecco's modified Eagle (DME) medium containing 10% (v/v) of fetal bovine serum at 37 °C in a humidified atmosphere of CO_2/air (1:9). For experiments with homogenates, cells were grown in 100-mm diameter plastic dishes, and for permeabilization experiments they were grown in 33-mm diameter dishes.

NRK Cell Homogenate Preparation. Cells were used for experiments when they were confluent and quiescent. For the [^{3}H]inositol homogenates, the cells were prelabeled for 72 h with [2-^{3}H]-*myo*-inositol (200 μCi/dish) added directly to the growth medium. The cells were scraped from the dish and resuspended in Hepes buffer composed of 120 mM KCl, 30 mM NaCl, 1 mM EGTA, 5 mM $MgCl_2$, and 50 mM Hepes, pH 7.1 (three 100-mm dishes were used for each time course). The cells were then homogenized by 12 strokes at 1200 rpm with a Thomas B Teflon homogenizer. Microscopic examination of the homogenate revealed that many of the cells were still intact but leaky as determined by trypan blue.

^{32}P-Phosphorylation of Homogenate and Chase. The homogenate was prepared from cells that were confluent and quiescent after 24 h of serum-free starvation. The homogenate containing 130 nM Ca^{2+}_{free} (buffered with EGTA) was preincubated at 25 °C for 5 min with [γ-^{32}P]ATP (35–50 μCi/mL, specific activity 5000 Ci/mmol) before being chased with 5 mM MgATP, either with or without GTPγS as indicated in the figure legends. Cell homogenates that had been prelabeled with [^{3}H]inositol were not labeled with [γ-^{32}P]ATP.

Experiments with Permeabilized Cells. NRK cells were seeded at 5×10^4 cells in 2 mL of medium into 33-mm dishes and used after 6–7 days, at which time the cells were confluent at densities of $(0.25–0.3) \times 10^7$ cells/plate. The cells were prelabeled for 48–72 h with [2-^{3}H]-*myo*-inositol (20 μCi/dish). The labeled medium was removed, and the cells were rinsed 3 times and incubated with phosphate-buffered saline (PBS), pH 7.4, for 30 min to remove as much as possible of the free [^{3}H]inositol. PBS was removed, and the cells were washed for 30 s in high-K^+ medium consisting of 120 mM KCl, 30 mM NaCl, 1 mM EGTA, 5 mM $MgCl_2$, 10 mM LiCl, 5 mM MgATP, 50 mM Hepes (pH 7.1), and 0.5 mM Ca^{2+} to give a free Ca^{2+} concentration of 130 nM and then treated by saponin (50 μg/mL) for 10 min in this high-K^+ medium. Saponin-treated cells were exposed to GTPγS for 5 min, and reactions were terminated by adding 1 mL of cold 15% trichloroacetic acid (TCA). The dishes were kept on ice for 30 min to extract the water-soluble inositol phosphates.

Extraction of Lipids and Thin-Layer Chromatography. Incubations of homogenates were terminated by removing samples (125 μL) at given times into 0.4 mL of $CHCl_3$/CH_3OH/HCl (200:400:5 v/v). The lipids were extracted for 30 min at 25 °C, followed by a phase split induced by adding 156 μL of $CHCl_3$ and 156 μL of 0.1 N HCl. The samples were then centrifuged at 12000*g* (Beckman Microfuge) for 2 min. The lower chloroform phase was removed, dried under N_2, resuspended in $CHCl_3$/CH_3OH/H_2O (2:1:0.01 v/v), and spotted onto potassium oxalate (1%) treated silica 60 TLC plates (Merck). For the permeabilized cells, the inositol lipids that remained on the dishes after removal of the inositol phosphates were extracted with 2 mL of $CHCl_3$/CH_3OH/concentrated HCl (200:100:1 v/v). The dishes were rinsed with an additional 1 mL of the same solvent, and the two extractions were combined. Phase split was induced by adding 1 mL of $CHCl_3$ and 1 mL of 0.1 N HCl, and the lower phase was removed, dried under N_2, resuspended in $CHCl_3$/CH_3OH/H_2O (2:1:0.01 v/v), and spotted onto the TLC plate. Phosphoinositides were separated by a one-dimensional chromatography system employing the solvent system $CHCl_3$/CH_3OH/4 N NH_4OH (9:7:2 v/v). Marker lipids were visualized by exposing the TLC plate to iodine vapor. The labeled lipids were detected by autoradiography, excised, and quantitated by liquid scintillation spectrophotometry. The identification of the phosphoinositides was confirmed by two-dimensional thin-layer chromatography [see Fleischman et al. (1986) for procedure]. This technique ensured that PIP was well separated from lyso-PI and lysophosphatidic acid, which migrate close to PIP in one-dimensional chromatography.

Table I: Estimates of Rate Constants for PI Turnover in the Presence and Absence of GTPγS[a]

conditions	k_1	k_2[b]	k_3	k_4	$k_3 + k_4$	k_5	k_6	k_7	k_8
[^{3}H]inositol flux									
−GTPγS	0.0012	0.13	0.69	0.025	0.72	<0.001	0.09	0.08	<0.01
+GTPγS	0.012*	1.4*	2.9*	0.65*	3.5*	<0.001	0.14	0.10	<0.01
[^{32}P]phosphate flux									
−GTPγS		0.07			1.0[c]				
+GTPγS		0.11			1.85*[c]				

[a] The constants (in min^{-1}) are those depicted in Scheme I, and the approximations made to determine the constants from the data in Figures 1 and 3 are discussed in the Appendix. All constants are pseudo-first-order rate constants in NRK cell homogenates determined at 25 °C in the presence of 5 mM MgATP, 120 mM KCl, 30 mM NaCl, 5 mM $MgCl_2$, 130 nM free Ca^{2+} (buffered with EGTA), and 50 mM Hepes, pH 7.1. The constants determined in the [^{32}P]phosphate flux experiment are the averages of the best fit constants determined from 12 separate experiments, each conducted with and without GTPγS. The constants from the [^{3}H]inositol flux experiments were from four separate experiments, each in the presence and absence of GTPγS. The asterisk indicates constants that are significantly altered from values in control experiments. [b] The values of k_2 given for the [^{3}H]inositol flux experiments are actually k_2' (see the Appendix, section A). [c] These values are actually for $k_3 + k_4'$, where $k_4' = k_4 + k_{-1}$ (see the Appendix, section B).

Analysis of Inositol Phosphates. The inositol phosphates were separated by anion-exchange chromatography on Dowex 1 (X8; formate form) as described by Berridge et al. (1983). Essentially, the ^{3}H-labeled phosphate esters were eluted sequentially by using 0.2 M ammonium formate/0.1 M formic acid (for IP_1), 0.4 M ammonium formate/0.1 formic acid (for IP_2), and 1.0 M ammonium formate/0.1 M formic acid (for IP_3). Separation of inositol 1,4,5-tris(phosphate) and inositol 1,3,4-tris(phosphate) was performed on a Partisil SAX 10 high-pressure anion-exchange column (Whatman), with [^{32}P]Ins-1,4,5-P_3 prepared from human red cell ghosts and [^{3}H]Ins-1,3,4-P_3 generously provided by Dr. P. Downes as standards. The flow rate was 2.5 mL/min, and fractions were collected every 0.3 min by using two linear ammonium formate gradients as described by Heslop et al. (1985). Water was passed through for 7 min; this was followed by a linear gradient over the next 24 min of 3.4 M ammonium formate buffered to pH 3.7, rising from water to 0.85 M ammonium formate. The second gradient over 12 min increased ammonium formate to 3.4 M.

Kinetic Analysis. See the Appendix.

Results

To determine whether guanine nucleotides stimulate breakdown of polyphosphoinositides in rat kidney fibroblast NRK cells, GTPγS was added to a homogenate of NRK cells that had been prelabeled to steady-state isotopic incorporation with [^{3}H]inositol. The cell homogenates were diluted into a buffer that maintained pH, Na^+, K^+, free calcium, and ATP concentrations at levels similar to those found in the cytosol of resting cells. Secondary effects due to changes in the level of the soluble catabolites of PI turnover, due to other soluble second messengers, or due to interaction of membrane-associated catabolites with soluble proteins were also minimized by the large dilution of these factors compared to their concentrations in intact cells. In addition, experiments were carried out at 25 °C to slow down the conversion between catabolites. Figure 1 shows that GTPγS (50 μM) increased the formation of labeled inositol phosphates. IP_3 increased more rapidly than the other two inositol phosphates and appeared to reach a steady-state level within 10–20 min. IP_2 and IP_1 continued to rise throughout the experiment. GTP caused a similar increase in the inositol phosphates although the response did not persist as long, and GDP was ineffective (data not presented). GTPγS stimulation was used for the kinetic analysis since it is more slowly hydrolyzed than GTP and provided an apparently continuous stimulation of PI turnover for 20 min at 25 °C. This prolonged stimulation simplified the analysis. Figure 2 shows the corresponding changes in the phosphoinositides on addition of GTPγS.

Scheme I: Phosphoinositide Metabolism Pathway[a]

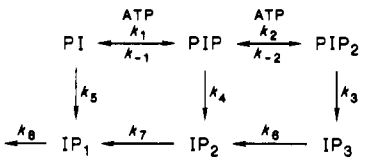

[a] The phosphoinositides PI, PIP, and PIP_2 are interconverted by kinases and phosphatases and hydrolyzed to the inositol phosphates IP, IP_2, and IP_3 by lipases. The rate constants indicated are pseudo-first-order constants that describe the relative rates of each step (see the Appendix, section A, and Table I for the values of these constants). The conversion of inositol 1,4,5-tris(phosphate) to inositol 1,3,4,5-tetrakis(phosphate) and inositol 1,3,4-tris(phosphate) is not depicted. See the Appendix, section C, for the rate constants for interconversion of these molecules.

Dilution of the cell homogenate into a buffer containing ATP and low Ca^{2+} with no GTPγS caused a slow decrease in both PIP and PIP_2. When GTPγS was included, a more rapid decrease in both lipids was observed although the eventual steady-state level of PIP and PIP_2 attained after 20 min was similar in the presence or absence of GTPγS. In the case of PIP_2 a transient 40% decrease at 2 min was observed, followed by a return to the control steady-state level by 10 min (Figure 2B). The amount of label present in [^{3}H]PI changed less than 15% during the 20-min incubation period with GTPγS (not shown).

In the Appendix, the solution to the differential equations that describe the simplest possible model for conversion between the intermediates in the PI turnover pathway is presented. The only complexity beyond the simple model in Scheme I needed to provide a good fit was the assumption that PIP kinase is activated with a lag time of several minutes following GTPγS addition. With this assumption, the equation provided an excellent fit to the data in Figures 1 and 2. A single set of rate constants provided a fit to the change in all five intermediates, PIP, PIP_2, IP_3, IP_2, and IP_1, which was within the standard deviation of the data. This result allows a comparison of the pseudo-first-order rate constants for the lipase, kinase, and phosphatase steps before and after stimulation with GTPγS. These rate constants are presented in Table I, and the lines drawn through the data in Figures 1 and 2 are theoretical curves from using the constants in Table I.

[^{3}H]IP_3 was resolved into Ins-1,4,5-P_3 and Ins-1,3,4-P_3 by HPLC, and the conversion between these intermediates was also modeled (Appendix). For this analysis we assumed conversion proceeded via the intermediate Ins-1,3,4,5-P_4 as shown by Hawkins et al. (1986) and Irvine et al. (1986). We have also demonstrated ATP-dependent conversion of exogenously added [^{32}P]Ins-1,4,5-P_3 to [^{32}P]Ins-1,3,4,5-P_4 and [^{32}P]Ins-1,3,4-P_3 by NRK fibroblast cell homogenates

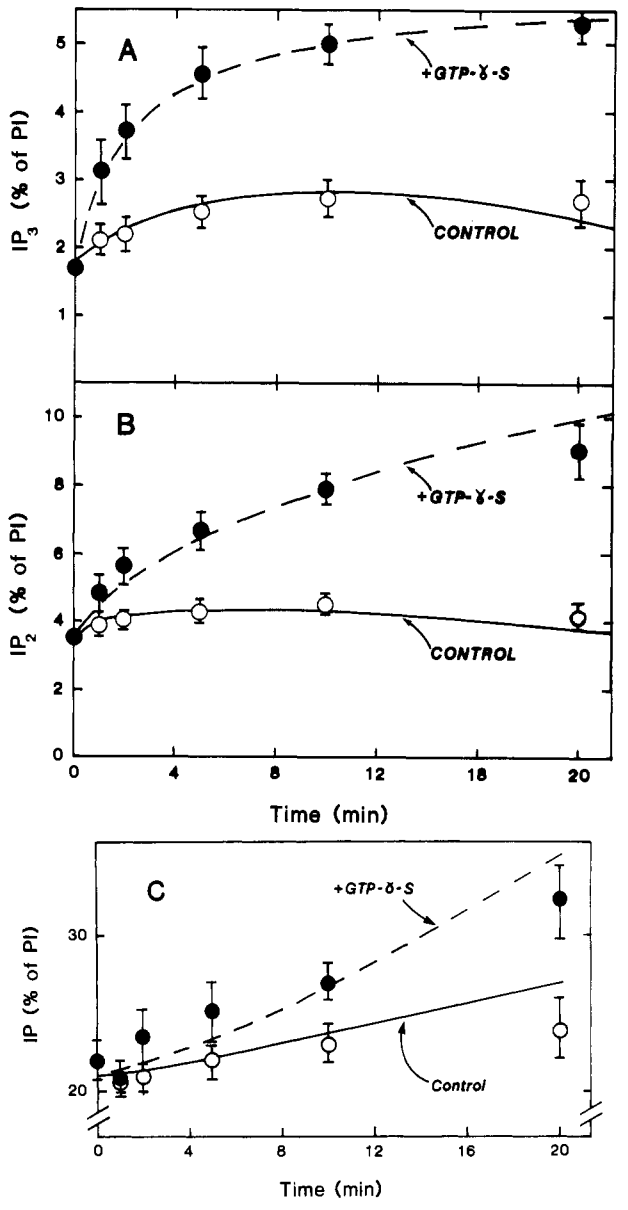

FIGURE 1: Time course of GTPγS effect on formation of water-soluble inositols in [^{3}H]inositol-labeled NRK cell homogenates. Homogenates were prepared from NRK cells prelabeled with [^{3}H]inositol for 72 h as described under Materials and Methods. At time zero the suspension was diluted into a Hepes buffer, pH 7.1, giving final concentrations of 120 mM KCl, 30 mM NaCl, 1 mM EGTA, 5 mM MgCl, 50 mM Hepes (pH 7.1), 5 mM MgATP, and 130 nM free Ca^{2+} with or without 50 μM GTPγS. At the indicated times, samples were removed and the lipids extracted and separated. The aqueous phase was used for water-soluble inositol determination and the lipid extract saved for phosphoinositide analysis (see Figure 2). Each point represents the mean of four separate experiments. The solid and dashed lines represent theoretical curves for inositol phosphate production in the absence and presence of GTPγS obtained by using the equations from section A of the Appendix and the constants in Table I. The error bars represent the standard error of the mean. The data are plotted as ratios of radioactivity in inositol phosphates to radioactivity in phosphatidylinositol to reduce errors due to transfer. The radioactivity in PI at each time point remained relatively constant at 53 000 ± 7000 cpm.

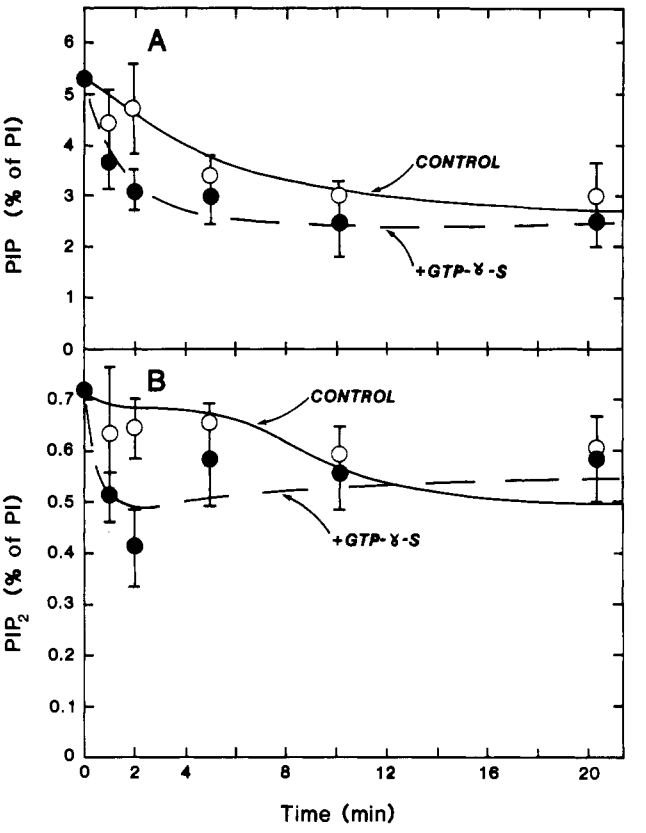

FIGURE 2: Effect of GTPγS on breakdown of [^{3}H]inositol-labeled phosphoinositides in NRK cell homogenates. This figure shows the corresponding changes in lipids during the experiments described in Figure 1. The phosphoinositides were separated as described under Materials and Methods. The solid and dashed lines are theoretical curves for breakdown in the absence and presence of GTPγS generated by using the equations in section A of the Appendix and the values of the rate constants given in Table I. The values are given as ratios to total radioactivity in PI that was scraped from the same thin layer. Since PI did not significantly change during the course of the experiment (53 000 ± 7000 cpm at each time point), this ratio reduced error due to pipetting.

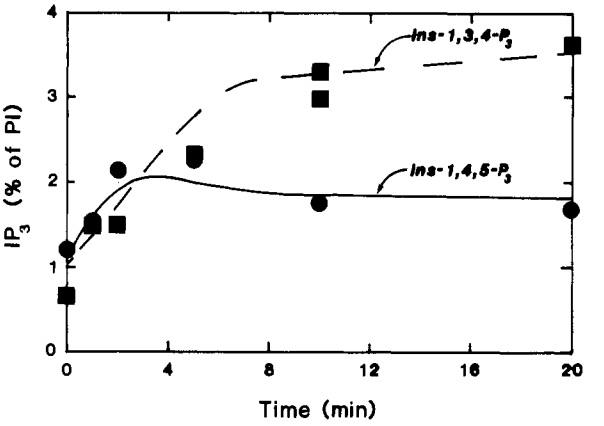

FIGURE 3: Time course for formation of [^{3}H]Ins-1,4,5-P_3 (●) and Ins-1,3,4-P_3 (■) in the presence of GTPγS. The experiment was performed as in Figure 1 except that a fraction of the water-soluble cell homogenate was subjected to HPLC analysis as described under Materials and Methods. The solid and dashed lines are theoretical curves drawn from using the equations and constants determined in section C of the Appendix. Data are expressed as ratio to counts in PI as described in the legend to Figure 1.

(Chahwala & Cantley, 1986). The data and the lines indicating the theoretical fit using the constants derived in the Appendix are presented in Figure 3. It is clear that Ins-1,4,5-P_3 peaks prior to Ins-1,3,4-P_3 in GTPγS-stimulated PI turnover, in agreement with results found in intact cells. Interestingly, the fit to the data indicates that, under the conditions of the in vitro stimulation, Ins-1,4,5-P_3 is converted to Ins-1,3,4,5-P_4 more rapidly than it is hydrolyzed to IP_2 (see section C of the Appendix). This result is consistent with the finding that the K_M for inositol 1,4,5-tris(phosphate) for the inositol-trisphosphate phosphatase (30 μM; Connolly et al., 1985) is much higher than the K_M for the inositol-1,4,5-tris-

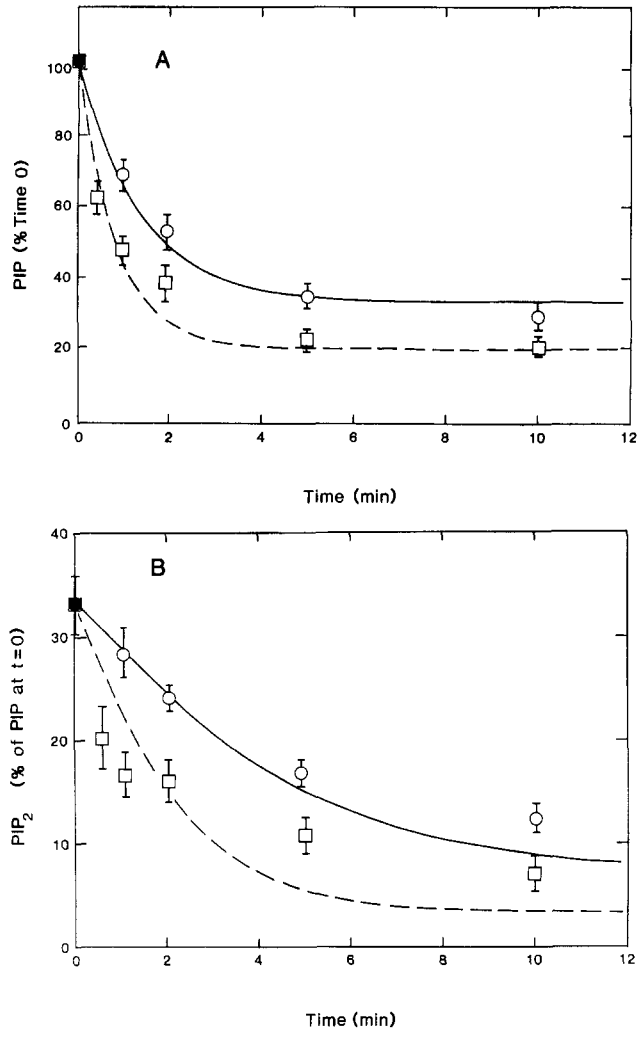

FIGURE 4: ^{32}P flux through PIP and PIP_2 in the absence and presence of GTPγS. NRK cell homogenates were phosphorylated for 5 min with [γ-^{32}P]ATP (50 μCi/mL) and then chased with 5 mM ATP for 10 min. The lipids were then extracted and analyzed by TLC as described under Materials and Methods. The data are the average of 12 separate experiments in the presence and absence of GTPγS. The radioactivity in PIP at time zero (average value of 8500 cpm over the 12 experiments) was normalized to 100, and radioactivity in PIP and PIP_2 at all other time points was expressed as a percentage of this value. The solid and dashed lines are theoretical curves for ^{32}P fluxes in the absence and presence of GTPγS, respectively, from using the equations in section B of the Appendix and the constants in Table I.

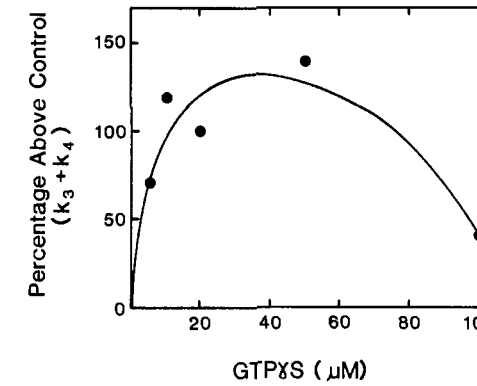

FIGURE 5: Effect of GTPγS concentration on phospholipase C activation ($k_3 + k_4$) in homogenates. Homogenates phosphorylated for 5 min with [γ-^{32}P]ATP (50 μCi/mL) were then chased with 5 mM ATP for 10 min in the presence of various concentrations of GTPγS. Time points were taken as in Figure 4, and the rate constants ($k_3 + k_4$) were obtained from best fit analysis of the data as described in section B of the Appendix.

Table II: Predicted Quantities of Diacylglycerol Derived from Breakdown of PI, PIP, and PIP_2[a]

conditions	PI hydrolysis	PIP hydrolysis	PIP_2 hydrolysis
control	<0.1	0.04	0.29
+GTPγS	<0.1	1.05	1.24

[a] The values were calculated by multiplying the rate constants for lipolysis of the respective lipids (from Table I) times the steady-state concentrations of the labile pools of each lipid (see the Appendix, section A). The numbers indicate the amount of diacylglycerol that should be produced from each lipid in 1 min as a percent of the total PI in the cell homogenate.

phosphate kinase (0.6 μM; Irvine et al., 1986).

A further check on the model in Scheme I and the rate constants determined from [^3H]inositol fluxes was provided by monitoring [^{32}P]phosphate fluxes through the intermediates PIP and PIP_2. Figure 4 shows that prelabeling of the homogenate with [γ-^{32}P]ATP for 5 min followed by a chase with cold ATP (5 mM) for 10 min results in a gradual decrease with time in the ^{32}P-labeled PIP and PIP_2. The rate constants for the kinase and lipase steps depicted in Scheme I were derived by fitting the equations in the Appendix to the values obtained for PIP and PIP_2 from the chase experiments. The theoretical curves for decline of radioactivity in PIP (Figure 4A) and PIP_2 (Figure 4B) in the absence and presence of GTPγS, from using the equations in section B of the Appendix, and the rate constants derived from the best fit to the data are also presented. Since changes in PIP and PIP_2 in response to GTPγS are smaller than the changes in inositol phosphates (see Figure 2), the rate constants are not as well determined from these data. However, these data, like the [^3H]inositol flux data, confirm an increase in the lipolysis of PIP and PIP_2 in response to GTPγS and also indicate an increase in PIP kinase (Table I). The [^{32}P]phosphate flux data also indicated that, under the conditions of the assay, degradation of PIP and PIP_2 by phosphatases was not significant (see the Appendix).

The concentration dependence of the GTPγS effect on the lipolysis steps (indicated by rate constants $k_3 + k_4$) was investigated in the experiment depicted in Figure 5. A maximal response was seen at 50 μM, and less activation was seen at higher concentrations.

In addition to the obvious effect of GTPγS on the lipolysis of PIP and PIP_2, two other important conclusions can be reached from the data in Table I. The first is that GTPγS has relatively little effect on the hydrolysis of PI. In the absence of GTPγS the relative rates of lipolysis of PI, PIP, and PIP_2 as estimated from the steady-state levels of these lipids and the rate constants k_5, k_4, and k_3 in Table I are 0.29 min^{-1} for PIP_2, 0.04 min^{-1} for PIP, and <0.1 min^{-1} for PI (Table II). This result predicts that less than 25% of the diacylglycerol comes from direct breakdown of PI under these conditions. When GTPγS was added, the lipolysis rates of PIP_2 and PIP increased by more than 4-fold, so that hydrolysis of these intermediates accounted for more than 95% of the PI turnover (Table II).

The second important observation is that GTPγS addition also caused an increase in the rates of the PI and PIP kinase steps. A comparison of the relative scales of the ordinates of Figures 1A and 2B demonstrates that within 5 min of GTPγS addition the increase in [^3H]IP_3 is approximately 20 times the decrease observed in [^3H]PIP_2. In addition, the steady-state level of PIP_2 reached after 5–10 min of GTPγS addition is not significantly different from that of the control despite the large differences seen in IP_3. Thus, the kinase step must be accelerated following GTPγS addition to maintain the PIP_2

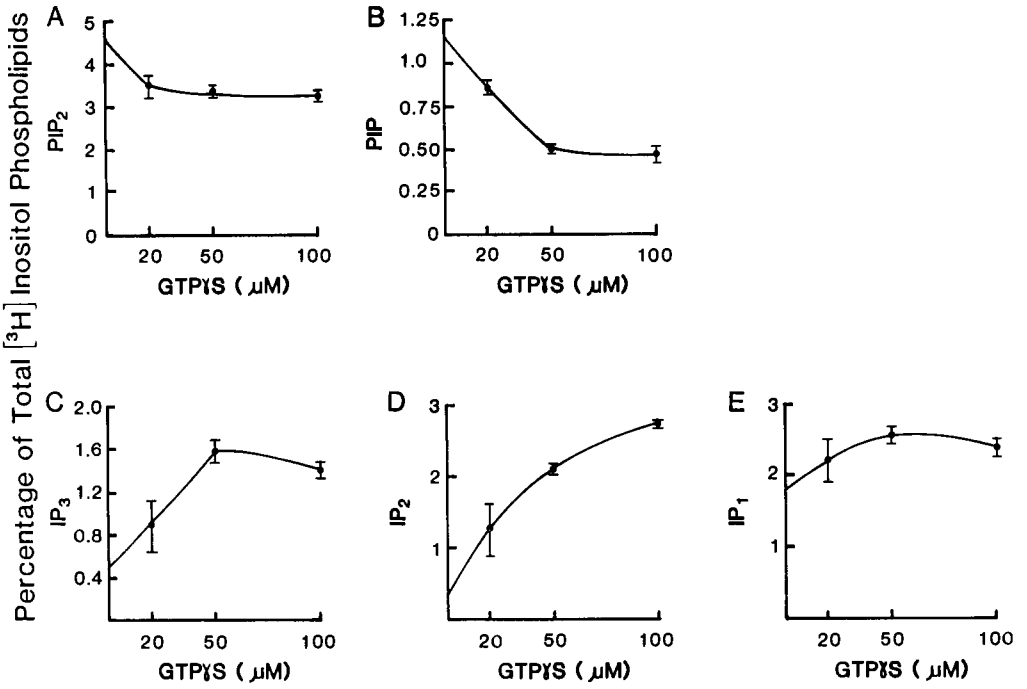

FIGURE 6: GTPγS-stimulated phosphoinositide breakdown in permeabilized NRK cells. NRK cells prelabeled with [^{3}H]inositol were permeabilized and exposed to various concentrations for 5 min. The levels of labeled inositol lipids and water-soluble inositol phosphates were determined as described under Materials and Methods. The bars indicate the standard error of the mean from three experiments.

level. Interestingly, with GTPγS addition we reproducibly found a rapid 40% decrease in PIP_2 followed by a recovery. This result indicates that the hydrolysis step is activated by GTPγS more rapidly than the kinase step and, as discussed above, requires that we include a lag time in activation of the PIP kinase to fit the data.

The rate constants for phosphatase action on IP_3, IP_2, and IP_1 were less well determined than those for the kinase and lipase steps. Unlike the lipase and kinase steps, both the enzymes and the substrates of the phosphatase steps are soluble. Thus, the large dilution in the cell homogenates compared with the concentrations that would be present in intact cells makes a comparison of the rates of these steps in homogenates to the rates in vivo tenuous at best. However, GTPγS appeared to have very little effect on these steps either from the fit to the data in Figures 1–3 or from direct measurement of [^{32}P]IP_3 breakdown (see the Appendix). Thus, the equations derived from Scheme I provide an excellent fit to all of the data by using the set of constants presented in Table I.

The effect of GTPγS on inositol lipid hydrolysis was also investigated in saponin-permeabilized cells. NRK cells, prelabeled with [^{3}H]inositol, were exposed, after permeabilization, to various concentrations of GTPγS (Figure 6). Only a small amount of the total [^{3}H]inositol incorporated into inositol lipids was accounted for by PIP_2 (4.5%) and PIP (1.2%). Addition of GTPγS caused a concentration-dependent decrease in PIP_2 and PIP with a concomitant increase in IP_3, IP_2, and IP_1. As with the phosphate flux in homogenized cells, the maximum effect of GTPγS was observed at 50 μM. At the highest concentration of GTPγS there was a decrease in PIP_2 by 27% and in PIP by 59% with a concomitant increase in IP_3 and IP_2 of 180% and 800%, respectively. These results are similar to those seen with cell homogenates, although the decrease in PIP is somewhat greater than that seen in Figure 2.

Discussion

The data presented in this article indicate that guanine nucleotide dependent breakdown of polyphosphoinositides occurs in NRK cells. Addition of GTPγS to homogenates of NRK cells stimulates phospholipase C, resulting in a more than 2-fold increase in the hydrolysis rate of PIP and PIP_2. In both the presence and absence of GTPγS, direct hydrolysis of PI appears to be small compared to the sum of the hydrolysis rates of PIP and PIP_2. Since the GTPγS-stimulated production of IP_3 is at least 10 times greater than the decrease seen in PIP_2, it appears that the PIP kinase step is also stimulated following GTPγS addition to homogenates. The kinase activation appears to lag behind the lipase activation as judged by the dip and recovery in the PIP_2 level following GTPγS addition (Figure 2B).

The concept that changes in phosphatidylinositol turnover are integrally involved in the action of a variety of hormones and growth factors is now well established (Berridge, 1984; Macara, 1985; Whitman et al., 1986a). In this paper we have attempted to model the kinetic mechanism for conversion between intermediates in PI turnover, using data derived from fluxes in cell homogenates stimulated with GTPγS. This GTP analogue was chosen because of its ability to cause a sustained stimulation of PI turnover, probably by binding to a GTP binding protein similar to proteins involved in regulation of adenosine cyclic 3′,5′-phosphate (cAMP) production. Evidence is accumulating to suggest that receptors linked to phosphoinositide changes are modulated via guanine nucleotide binding regulatory protein(s). Although a role for such N proteins has been shown in various cell types (see below), guanine nucleotide dependent hydrolysis of PIP_2 has not been reported previously in a fibroblast cell line such as NRK cells, where growth factor mediated PI turnover can be connected with cell growth.

A major question in receptor-mediated PI turnover concerns the relative contribution of the polyphosphoinositide intermediates to the total mass of PI breakdown. This question is of particular importance in determining the roles of the PI and PIP kinases in generating substrate for diacylglycerol production. (The importance of these kinases for IP_3 production is obvious.) Berridge (1983) and Downes and Wusteman (1983) have proposed that essentially all of the

agonist-induced PI breakdown occurs by conversion of PI to PIP and then to PIP_2 prior to hydrolysis by phospholipase C [for review see Berridge (1984)]. However, this hypothesis has recently been questioned by Majerus and colleagues (Wilson et al., 1985; Majerus et al., 1985), who have proposed that, on the basis of kinetic analysis in platelets, there is a direct phospholipase C hydrolysis of PI. In addition, Dixon and Hokin (1985) have provided evidence of phospholipase C breakdown of PI in pancreatic minilobules through identification of inositol cyclic 1,2-phosphate. These conclusions were derived from studies employing standard pulse–chase experiments using [^{32}P]phosphate or [^{3}H]inositol label in intact cells. Because of the rapid rate at which inositol polyphosphates are degraded by phosphatases in intact cells, it is difficult to determine the immediate source of the inositol 1-phosphate in such experiments.

In order to gain a better understanding of what steps in this complex pathway are affected by GTPγS, we monitored the concentration of seven of the intermediates (PI, PIP, PIP_2, Ins-1,4,5-P_3, Ins-1,3,4-P_3, IP_2, and IP) following GTPγS addition to a medium containing ATP, Mg^{2+}, and free Ca^{2+} concentrations similar to those in vivo. We also used two different labeling techniques to confirm the values of the rate constants. Our conclusion is that in fibroblasts GTPγS stimulates preferential hydrolysis of the polyphosphoinositides rather than direct hydrolysis of PI. Wilson et al. (1984) have shown that purified phospholipase C has a preference for polyphosphoinositides over PI in the presence of submicromolar concentrations of free calcium. However, they point out that because of the overwhelming excess of PI over PIP and PIP_2, direct PI hydrolysis should still be much greater than PIP or PIP_2 hydrolysis. Using the rate constants from Table I and the relative steady-state levels of PI, PIP, and PIP_2 in the homogenates, we estimate (Table II) that, in the presence of GTPγS, PIP_2 hydrolysis accounts for at least 10 times as much diacylglycerol as direct PI breakdown despite the 100-fold excess of PI over PIP_2. These results can be compared to the effect of GTPγS on the relative rates of PI and PIP_2 breakdown in membranes from blowfly salivary glands (Litosch & Fain, 1985). In those experiments, exogenously added PIP_2 was hydrolyzed about 5 times more rapidly than exogenously added PI, and GTPγS caused a 2-fold increase in hydrolysis of the former but only about a 30% increase in hydrolysis of the latter. These three studies differ in tissue source, in use of exogenously added vs. endogenous substrates, and in use of membrane-associated vs. purified, soluble phospholipase C. Further work will be necessary to determine whether the greater PIP_2 specificity of the GTPγS-stimulated lipase compared to that of the purified sheep seminal vesicle enzyme is due to differences in the enzyme or substrate presentation.

The mechanism by which the PI and PIP kinases are activated to replenish the hydrolyzed PIP and PIP_2 is not clear. That the kinases are activated is obvious since the accumulation of [^{3}H]IP_3 and IP_2 greatly exceeded the starting level of radioactivity in the parent lipids PIP_2 and PIP (see Figures 1 and 2). The only simple explanation for this result is that the labeled polyphosphoinositides are constantly being replenished from the labeled PI pool. Immediately following the GTPγS addition to homogenates, a rapid decrease in PIP_2 occurred, followed by a recovery to almost the initial level. It is interesting to compare the kinetics of the change in [^{3}H]PIP_2 caused by GTPγS with hormone effects on intact cells. Platelet-derived growth factor (PDGF) in human fibroblasts (Chu et al., 1985), concanavalin A in thymocytes (Taylor et al., 1984), vasopressin in hepatocytes (Creba et al., 1983), and

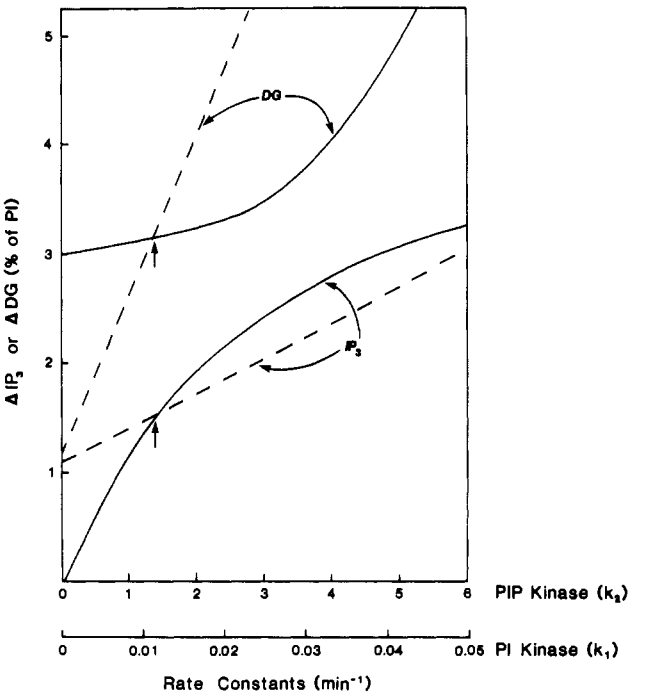

FIGURE 7: Theoretical curves predicting the effect of varying PI (dashed lines) or PIP kinase (solid lines) rates on the levels of IP_3 and DG produced 2 min after stimulation with GTPγS. The IP_3 and DG were calculated by using the equations in section A of the Appendix. For the dashed lines, the PI kinase rate constant was varied while PIP kinase and all other steps in the pathway of Scheme I were held constant at the values reported in the presence of GTPγS in Table I. For the solid lines, the PIP kinase rate was varied with PI kinase and all other constants fixed at the values reported in the presence of GTPγS in Table I. The increase in IP_3 determined experimentally and the predicted increase in DG from the sum of IP_3 + IP_2 + IP measured at 2 min after GTPγS addition are indicated by the arrows where the dashed and solid lines cross. Degradation of DG was not incorporated into the model.

fMet-Leu-Phe in neutrophils (Della Bianca et al., 1986) are all known to cause a rapid breakdown of PIP_2 followed by resynthesis. With fMet-Leu-Phe stimulation, the PIP_2 level rises above the starting level and PIP rises throughout the stimulation with no decrease, suggesting that both PI and PIP kinase activities are increased. The fact that GTPγS induces a similar pattern of PIP_2 breakdown and resynthesis suggests that the concentration of PIP_2 itself may be important in regulating PIP kinase activity (rather than direct effect of receptors on the kinase). In vitro, PIP_2 has been shown to inhibit the activity of PIP kinase (Rooijen et al., 1985). However, using partially purified PIP kinase from murine erythroleukemia cells, we have found that PIP_2 is only an effective inhibitor when present at concentrations equal to the PIP concentration and that the inhibition shows hyperbolic saturation (Schultz et al., 1986). Because of the relatively large PIP to PIP_2 ratio in the cell homogenates, it seems unlikely that the small decrease in PIP_2 observed (Figure 2) would have a significant effect on PIP kinase activity.

The equations in the Appendix can be used to predict the effect of varying the activity of the PI and PIP kinases on the second messengers IP_3 and DG. In Figure 7 the predicted increase in DG and IP_3 at 2 min after addition of GTPγS is plotted as a function of the pseudo-first-order rate constant for PI kinase. All other rate constants were fixed at their values given in Table I. The arrows indicate the increase in IP_3 measured experimentally and the predicted increase in DG estimated from the increase in the sum of IP, IP_2, and IP_3 measured experimentally at 2 min after GTPγS addition. As

can be seen, both DG and IP_3 increase linearly, but the slope of the increase in DG is much steeper. This results because some of the PIP formed can be hydrolyzed to DG directly without conversion to PIP_2. The lines do not intercept the ordinate axis at 0, since in the absence of PI kinase activity, the existing PIP at the time of stimulation can be converted to DG and PIP_2. However, the difference between the amount of DG formed in 2 min with a PI kinase rate of 0.014 min^{-1} (the value determined experimentally in the presence of GTPγS) and that with a rate of 0 is approximately 3-fold.

Varying the PIP kinase activity has a very different effect on DG and IP_3 levels. As can be seen in Figure 7, the level of IP_3 at 2 min after GTPγS addition is very sensitive to the PIP kinase rate while the amount of DG formed is relatively insensitive in the range of the rate constant observed experimentally. This phenomenon is a consequence of the fact that in the absence of PIP kinase activity the labile pool of PIP_2 is hydrolyzed well before the 2-min time point and no new IP_3 can be produced. However, DG can still be formed from PIP. Thus, by individually varying the PI and PIP kinases, the ratio of IP_3 to DG produced in response to a hormone or growth factor could be dramatically varied. This treatment of course does not consider the additional complexity that would be introduced by the change in free calcium that would occur in an intact cell. In any event, these theoretical curves support the proposal which has been made that certain oncogenes mediate cell transformation at least partially by activating PI and PIP kinases (Whitman et al., 1985, 1986a,b; Kaplan et al., 1986).

GTPγS also stimulated an increase in IP_3, IP_2, and IP in saponin-permeabilized NRK cells. Interestingly, under these conditions, the increase in IP_3 and IP_2 was accompanied by quantitatively similar decreases in PIP_2 and PIP, suggesting that in saponin-permeabilized cells no significant kinase activation occurs. This result can partially be explained by the removal of PIP kinase from the membrane under these conditions (Schulz et al., 1986).

The question of what GTP binding protein is involved in activation of phospholipase C remains to be determined. There is now evidence that guanine nucleotide binding proteins play an important role in the link between Ca^{2+}-mobilizing receptors and the PIP_2 phospholipase C in a variety of tissues. Gomperts (1983) and Haslam and Davidson (1984) have shown that GTPγS can increase Ca^{2+}-mediated histamine release from permeabilized rat mast cells and [^{14}C]serotonin secretion from permeabilized human platelets, respectively. Cockcroft and Gomperts (1985) reported GTPγS-stimulated breakdown of PIP_2 in human neutrophil plasma membranes at concentrations of Ca^{2+} pertaining in unstimulated cells. Lucas et al. (1985) have reported that direct stimulation by thyrotropin-releasing hormone of PIP_2 breakdown in GH_3 cell membranes is potentiated by GTP. Pertussis toxin, which inactivates guanine nucleotide binding proteins (N_i and N_0), can inhibit fMet-Leu-Phe-induced increase in Ca^{2+} in neutrophils (Okajima & Ui, 1984) and Ca^{2+}-dependent histamine release from mast cells (Nakamura & Ui, 1985). However, Masters et al. (1985) observed that treatment with pertussis toxin of cultured 1321 N1 human astrocytoma cells had no effect on the muscarinic receptor mediated stimulation of PIP_2 hydrolysis. They suggested that muscarinic receptors are not coupled to N_i in terms of PIP_2 breakdown. We too have found no effect of pertussis toxin treatment of NRK cells on GTPγS-stimulated PIP_2 breakdown (Chahwala et al., unpublished results). Gilman (1983) has proposed that there may be a family of different guanine nucleotide binding regulatory proteins involved in mediating a wide variety of cellular responses. It is possible that in some cells more than one GTP binding protein mediates PI turnover so that the GTP effects seen in vitro represent stimulation through more than one system. The possibility that the protein product of the *ras* oncogene may be involved in regulation of phospholipase C has been suggested from steady-state levels of intermediates of PI turnover in transformed cells (Fleischman et al., 1986). The question of what, if any, GTP binding protein mediates growth factor responses remains to be resolved.

Acknowledgments

We thank Philip Rosoff and Malcolm Whitman for many helpful discussions. We especially thank Anne Burgess for both intellectual and technical input.

Appendix

Rate Equations for Phosphatidylinositol Turnover. (A) [^{3}H]Inositol Steady-State Labeling Experiment. The following simplifying assumptions were made in deriving the time dependence of [^{3}H]IP_3, [^{3}H]IP_2, and [^{3}H]IP_1 production from homogenates of cells that had been labeled to steady state with [^{3}H]inositol: (1) The pathway for production of IP_3, IP_2, and IP_1 indicated in Scheme I was assumed. The reverse reactions of the steps for rate constants k_3, k_4, k_5, k_6, k_7, and k_8 were assumed to have negligible rate constants since these reverse reactions are not detectable in cell homogenates. The phosphatase steps indicated by rate constants k_{-1} and k_{-2} were also assumed to be negligible for this derivation. The validity of this assumption is discussed in section B. (2) The PI concentration was treated as a constant since less than 20% of the PI was consumed during the 20-min incubation period. (3) The rates of the PI kinase, PIP kinase, and phospholipase C catalyzed steps as well as the IP_3, IP_2, and IP_1 phosphatase steps were assumed to be first order in substrate concentration (i.e., operating below the K_M). Thus, the rate constants in Scheme I are actually ratios of V_{max} to K_M for the respective enzymes. This assumption is likely to be true for the IP_3, IP_2, and IP_1 phosphatase steps since the substrate concentrations are considerably more dilute in cell homogenates than in the intact cell. The affinities of the PI and PIP kinases and of phospholipase C for their respective lipid substrates are more difficult to evaluate. Preliminary results with partially purified PI and PIP kinases from brain indicate that, at in vivo lipid ratios, PI and PIP are at or below their K_M values for these enzymes. All the substrate concentrations are expressed as percentages of PI in the homogenate.

With these assumptions, the time dependence of PIP production is defined by

$$[PIP] = [PIP^{ss}] + [X0]e^{-(k_2+k_4)t} \qquad (A1)$$

where $[PIP^{ss}] = [PIP^{ss*}] + k_1[PI]/(k_2 + k_4)$ is the steady-state concentration of PIP at times much greater than the reciprocal of rate constants $k_2 + k_4$ and $[PIP^{ss*}]$ is the fraction of PIP that is not available for turnover; $[X0] = [PIP^0] - [PIP^{ss}]$, and $[PIP^0]$ is the concentration of PIP at time zero. In all the following derivations, the superscripts 0 and ss refer to the substrate concentration at time zero and at steady state, respectively. The other constants are defined in Scheme I. Equation A1 was fit to the data obtained in the presence and absence of GTPγS in Figure 2A by using a nonlinear least-squares program. $[PIP^0]$ was assigned the value measured at time zero (expressed as percent of counts in PI; i.e., $[PIP^0] = 5.2$ and $[PI] = 100$). Since the [^{32}P]phosphate flux experiments indicate that approximately 30% of the PIP is not available for degradation (see section B), $[PIP^{ss*}]$ was assigned

the value of $0.30[PIP^0]$. The sum $k_2 + k_4$ was determined from the fit to be 0.2 min^{-1} in the absence of GTPγS and 0.7 min^{-1} in the presence of GTPγS. The only other unknown was k_1, which was determined from the best fit value for $[PIP^{ss}]$ to be 0.0012 min^{-1} in the absence of GTPγS and 0.012 min^{-1} in the presence of GTPγS. Assigning $[PIP^{ss*}]$ the value of $0.30[PIP^0]$ had little effect on the best fit values determined for $k_2 + k_4$, but it did improve the fit to the data compared to an assignment of 0.

The time dependence of PIP_2 hydrolysis is defined by

$$[PIP_2] = [PIP_2^{ss}] + [X1]e^{-(k_2+k_4)t} + [X2]e^{-k_3t} \quad (A2)$$

where

$$[PIP_2^{ss}] = [PIP_2^{ss*}] + k_1k_2[PI]/k_3(k_2 + k_4)$$
$$[X1] = k_2[X0]/[k_3 - (k_2 + k_4)]$$
$$[X2] = [PIP_2^0] - [PIP_2^{ss}] - [X1]$$

The only constants from this equation not previously determined from the fit of eq A1 to the PIP data are k_2 and k_3. As discussed below, k_3 was more accurately determined from the IP_3 data, and an iterative procedure was used to determine that the best fit value of k_3 determined from eq A3 below provided the best fit for eq A2 (values of 0.69 min^{-1} in the absence of GTPγS and 2.9 min^{-1} in the presence of GTPγS were used for the fit). Thus, the PIP_2 data were used primarily to determine k_2. $[PIP_2^{ss*}]$ was assigned the value $0.30[PIP_2^0]$ to account for the 30% of PIP_2 that fails to turn over in the $[^{32}P]$phosphate flux experiments (see below). The best fit value for k_2 was approximately 0.1 in the absence of GTPγS and 0.4 in the presence of GTPγS. However, eq A2 failed to fit the rapid decrease and recovery in PIP_2 that occurred during the first 5 min after addition of GTPγS. This rapid dip and recovery was seen in all four experiments performed. A modification of eq A2, in which k_2 was replaced by $k_2'(1 - e^{-t/T})$, allowed a fit to the data well within the standard deviation (see dashed line in Figure 1B). This equation assumes that PIP kinase is activated with a 4-min lag time (i.e., T = 4 min) following addition of GTPγS plus ATP to the cell homogenate. The value of k_2' determined from the fit was 0.13 min^{-1} in the absence of GTPγS and 1.4 min^{-1} in the presence of GTPγS. The values determined for the other constants in eq A1–A5 were not significantly altered by the choice of a fixed value or a time-dependent value for k_2 in the fitting procedure. For consistency the time-dependent quantity $k_2'(1 - e^{-t/T})$ was used in place of k_2 in the fits used to determine the other constants in Table I and in drawing the theoretical lines in Figure 1.

The time course of IP_3 production is defined by

$$[IP_3] = [IP_3^{ss}] + [X3]e^{-(k_2+k_4)t} + [X4]e^{-k_3t} + [X5]e^{-k_6t} \quad (A3)$$

where

$$[IP_3^{ss}] = k_1k_2[PI]/k_6(k_2 + k_4)$$
$$[X3] = k_3[X1]/[k_6 - (k_2 + k_4)]$$
$$[X4] = k_3[X2]/(k_6 - k_3)$$
$$[X5] = [IP_3^0] - [IP_3^{ss}] - [X3] - [X4]$$

The curvature of the IP_3 data is primarily determined by the constants k_6 and k_3. As discussed above, an iterative nonlinear least-squares fitting procedure was used to ensure that the value of k_2 determined from eq A2 provided the best fit for eq A3. The rate constants determined were k_3 = 0.69 and k_6 = 0.09 in the absence of GTPγS and k_3 = 2.9 and k_6 = 0.14 in the presence of GTPγS (all in units of min^{-1}). By use of the values of k_2 and $k_2 + k_4$ determined above, the value of k_4 can be calculated in the presence and absence of GTPγS to be 0.025 and 0.6 min^{-1}, respectively.

The time dependence of IP_2 production is defined by

$$[IP_2] = [IP_2^{ss}] + [X6]e^{-(k_2+k_4)t} + [X7]e^{-k_3t} + [X8]e^{-k_6t} + [X9]e^{-k_7t} \quad (A4)$$

where

$$[IP_2^{ss}] = k_1[PI]/k_7$$
$$[X6] = \{k_6k_3k_2 + k_4[k_6 - (k_2 + k_4)][k_3 - (k_2 + k_4)]\} \times [X0]/\{[k_7 - (k_2 + k_4)][k_6 - (k_2 + k_4)][k_3 - (k_2 + k_4)]\}$$
$$[X7] = k_6[X4]/(k_7 - k_3) \qquad [X8] = k_6[X5]/(k_7 - k_6)$$
$$[X9] = [IP_2^0] - [IP_2^{ss}] - [X6] - [X7] - [X8]$$

All the constants in eq A4 except k_7 were determined above. By fitting eq A4 to the data in Figure 1B and allowing k_7 to vary, the best fit value was 0.08 min^{-1} in the absence and 0.1 in the presence of GTPγS.

The time dependence of IP_1 production is defined by

$$[IP_1] = [IP_1^{ss}] + [Y1]e^{-(k_2+k_4)t} + [Y2]e^{-k_3t} + [Y3]e^{-k_6t} + [Y4]e^{-k_7t} + [Y5]e^{-k_8t} \quad (A5)$$

where

$$[IP_1^{ss}] = (k_1 + k_5)[PI]/k_8$$
$$[Y1] = k_7[X6]/[k_8 - (k_2 + k_4)]$$
$$[Y2] = k_7[X7]/(k_8 - k_3)$$
$$[Y3] = k_7[X8]/(k_8 - k_6) \qquad [Y4] = k_7[X9]/(k_8 - k_7)$$
$$[Y5] = [IP_1^0] - [IP_1^{ss}] - [Y1] - [Y2] - [Y3] - [Y4]$$

Constants k_8 and k_5 are the only rate constants in eq A5 that were not previously determined. The best fit of this equation to the data in Figure 1C is obtained when k_8 is less than 0.01 min^{-1} and k_5 is less than 0.001 min^{-1} both in the presence and in the absence of GTPγS. This result is obtained because essentially all the PI breakdown can be accounted for by the increase in $IP_3 + IP_2 + IP_1$, indicating that IP_1 phosphatase (represented by k_8) is less active than the IP_3 and IP_2 phosphatases. The fact that the IP phosphatase step is the slowest in this pathway is in agreement with in vivo results. In addition, essentially all the IP_1 can be accounted for by the breakdown of IP_2, suggesting that very little direct lipolysis of PI occurs under these conditions (i.e., k_5 is small compared to k_1; see Table I). Also, in agreement with the observation that GTPγS has no effect on the rate of hydrolysis of exogenously added $[^{32}P]IP_3$ (data not shown), the rate constants for the three phosphatase steps k_6, k_7, and k_8 were not affected by the presence or absence of GTPγS. All the rate constants are summarized in Table I. The solid and dashed lines through the data in Figures 1 and 2 are theoretical curves from using eq A1–A5 and the constants in Table I.

(B) $[^{32}P]$Phosphate Flux Experiment. Unlike the $[^3H]$-inositol labeling experiments, $[^{32}P]$phosphate labeling (Figure 4) was done as a pulse and chase. The change in radioactivity in an intermediate was due to replacement of labeled phosphate with unlabeled phosphate subsequent to the addition of excess unlabeled ATP. The concentration of unlabeled ATP (5 mM) and all other conditions were the same as those used in the $[^3H]$inositol labeling experiment. Only two assumptions were made in solving the time dependence of ^{32}P flux through PIP and PIP_2. (1) The mechanism in Scheme I was assumed. Two paths for degradation of PIP and PIP_2 were included: phospholipase C catalyzed hydrolysis was represented by rate

constants k_3 and k_4, and phosphatase hydrolysis was represented by rate constants k_{-1} and k_{-2}. Although the phosphatase pathway was included in the derivations below, the fits of the equations to the data indicate that this pathway does not account for a significant fraction of the degradation. (2) All steps were assumed to be first order in substrate concentration. The validity of this assumption was discussed in section A.

With these assumptions the time dependences of phosphate flux through PIP and PIP_2 are given by

$$[PIP_2] = [PIP_2^{ss}] + \{k_2/(\lambda_1 - \lambda_2)\}[Y1]e^{-\lambda_1 t} + \{k_2/(\lambda_1 - \lambda_2)\}[Y2]e^{-\lambda_2 t} \quad (B1)$$

$$[PIP] = [PIP^{ss}] + \{(k_3 + k_{-2} - \lambda_1)/(\lambda_1 - \lambda_2)\}[Y1]e^{-\lambda_1 t} + \{(k_3 + k_{-2} - \lambda_2)/(\lambda_1 - \lambda_2)\}[Y2]e^{-\lambda_2 t} \quad (B2)$$

where

$$[Y1] = [PIP_2^0](k_3 + k_{-2} - \lambda_2)/k_2 - [PIP^0] + k_1[PI^0]\lambda_2/Z$$

$$[Y2] = -[PIP_2^0](k_3 + k_{-2} - \lambda_2)/k_2 + [PIP^0] - k_1[PI^0]\lambda_1/Z$$

$$\lambda_1 = 0.5(k_3 + k_{-2} + k_2 + k_4 + k_{-1}) - 0.5\sqrt{(k_3 + k_{-2} + k_2 + k_4 + k_{-1})^2 - 4Z}$$

$$\lambda_2 = 0.5(k_3 + k_{-2} + k_2 + k_4 + k_{-1}) + 0.5\sqrt{(k_3 + k_{-2} + k_2 + k_4 + k_{-1})^2 - 4Z}$$

$$Z = k_2k_3 + (k_4 + k_{-1})(k_3 + k_{-2})$$

The values of $[PIP^{ss}]$ and $[PIP_2^{ss}]$, the relative amounts of ^{32}P in PIP and PIP_2 at long times after the chase with unlabeled ATP, should be 0 if the isotopic dilution is infinite and all the PIP and PIP_2 molecules that get labeled are accessible to phospholipase C. In addition, $k_1[PI^0]$ should also be 0 if an insignificant amount of [^{32}P]ATP is available for further phosphorylation. However, both [PIP] and $[PIP]_2$ leveled off at nonzero values (see Figure 4), indicating that a small pool of PI is available for phosphorylation but not hydrolysis (i.e., accounting for approximately 30% of the PIP_2 formed). The possibility that significant ^{32}P flux still occurs following the ATP dilution because of a relatively high K_M(ATP) for the PI and PIP kinases can be eliminated since we have determined the K_M's for ATP for the major PI and PIP kinases in these cells (Schulz et al., 1986; Whitman et al., 1986b). Thus, $[PIP^{ss}]$ and $[PIP_2^{ss}]$ were treated as constants to account for a lipase-insensitive pool.

In fitting the above equations to the experimental data, $[PIP^0]$ and $[PIP_2^0]$ were taken as the radioactivity in PIP and PIP_2 immediately before addition of unlabeled ATP; $[PIP^{ss}]$ and $[PIP_2^{ss}]$ were the values after no further change in radioactivity was observed with time (i.e., $t > 20$ min). Since k_4 and k_{-1} always appear in the equations as a sum, this sum was treated as a single constant, k_4'. The constants k_1 and $[PI^0]$ appear throughout the equations as a product and were designated by the pseudo rate constant $k_1' = k_1[PI^0]$. Also, by combining eq B1 and B2, it may be shown that $k_2 = (k_3 + k_{-2})[PIP^{ss}]/[PIP_2^{ss}]$.

Thus, only four independent constants are unknown in eq B1 and B2 (k_1', k_{-2}, k_3, and k_4'). These four constants were allowed to vary according to a nonlinear least-squares program that simultaneously fit the two equations to the two sets of data (for radioactive label in PIP and PIP_2 as a function of time after the chase with unlabeled ATP; see Figure 4 for the fit). The best fit value for k_{-2} was consistently less than $0.1k_3$ in 12 separate experiments and was therefore assumed to be negligible. This result suggests that hydrolysis of PIP_2 by phosphatase is not significant in NRK cell homogenates under the conditions of our assays (high ATP and low Ca^{2+}). Although the relative values of k_3 and k_4' obtained from fits of the equations to data obtained on separate days varied considerably, the sum of these two constants (which represents the net loss of isotope from the two intermediates) was relatively reproducible from day to day ($k_3 + k_4' = 1.0 \pm 0.13$ min^{-1}; see Table I). The value of $k_3 + k_4'$ obtained from the ^{32}P flux experiments was very similar to the value of $k_3 + k_4$ obtained from the [^{3}H]inositol flux experiment ($k_3 + k_4 = 0.72$ min^{-1}; Table I). Since k_4' is actually the sum of k_4 and k_{-1}, then if k_{-1} were a relatively large rate (i.e., if a significant hydrolysis of PIP by a phosphatase were occurring), $k_3 + k_4'$ obtained from the ^{32}P flux would be much larger than $k_3 + k_4$ obtained from [^{3}H]inositol flux measurements. This is clearly not so.

Also presented in Table I is the effect of GTPγS on the rate constants. All experiments were conducted by adding GTPγS to one fraction of the previously labeled membranes along with the unlabeled ATP so that the control and GTPγS experiments could be followed in parallel. The sum $k_3 + k_4'$ increased by 85% ± 15% in 12 separate experiments. An increase in k_2 was also seen, but the error in this constant was approximately equal to the increase. The fits were even less sensitive to the value of k_1'.

(C) Conversion of Inositol 1,4,5-Tris(phosphate) to Inositol 1,3,4-Tris(phosphate). In section A the treatment of IP_3 did not resolve the two isomers IP_3(1,4,5) and IP_3(1,3,4). It has been shown that conversion of IP_3(1,4,5) to IP_3(1,3,4) occurs by the mechanism (Hawkins et al., 1986; Irvine et al., 1986)

$$IP_3(1,4,5) + ATP \xrightarrow{k_9} IP_4(1,3,4,5) + ADP \xrightarrow{k_{10}} IP_3(1,3,4) + P_i$$

These additional intermediates can easily be incorporated into the equations derived in section A by assuming that the two steps indicated by rate constants k_9 and k_{10} are irreversible and by assuming that the intermediate IP_4 quickly reaches a steady state. The former assumption is justified by the high ATP/ADP ratio in the in vitro assay. The latter assumption is supported by the very low level of IP_4 (or higher phosphorylated forms of inositol) detected in the in vitro assays (Chahwala, unpublished results). From the steady-state assumption, $[IP_3(1,4,5)]k_9 = [IP_4]k_{10}$. The time dependence of $[IP_3(1,4,5)]$ can then be described by

$$[IP_3(1,4,5)] = [IP_3(1,4,5)^{ss}] + [Z1]e^{-(k_2+k_4)t} + [Z2]e^{-k_3 t} + [Z3]e^{-(k_6+k_9)t} \quad (C1)$$

where

$$[IP_3(1,4,5)^{ss}] = k_1k_2[PI]/(k_6 + k_9)(k_2 + k_4)$$

$$[Z1] = k_3[X1]/[(k_6 + k_9) - (k_2 + k_4)]$$

$$[Z2] = k_3[X2]/[(k_6 + k_9) - k_3]$$

$$[Z3] = [IP_3(1,4,5)^0] - [IP_3(1,4,5)^{ss}] - [X3] - [X4]$$

and the other constants are defined in section A.

This equation is identical with eq A3 except that k_6 is replaced by the sum $k_6 + k_9$. This is because IP_3(1,4,5) can be converted to two different species, IP_2 or IP_4.

The time dependence of IP_3(1,3,4) concentration is described by

$$[IP_3(1,3,4)] = [IP_3(1,3,4)^{ss}] + [Z4]e^{-(k_2+k_4)t} + [Z5]e^{-k_3 t} + [Z6]e^{-(k_6+k_9)t} + [Z7]e^{-(k_6')t} \quad (C2)$$

where

$$[IP_3(1,3,4)^{ss}] = k_9k_1k_2[PI]/k_6'(k_6 + k_9)(k_2 + k_4)$$

$$[Z4] = k_9[Z1]/[k_6' - (k_2 + k_4)]$$

$$[Z5] = k_9[Z2]/(k_6' - k_3)$$

$$[Z6] = k_9[Z3]/[k_6' - (k_6 + k_9)]$$

$$[Z7] = [IP_3(1,3,4)^0] - [IP_3(1,3,4)^{ss}] - [Z4] - [Z5] - [Z6]$$

and k_6' is the rate constant for conversion of $IP_3(1,3,4)$ to IP_2. Equations C1 and C2 were fit to the $IP_3(1,4,5)$ and $IP_3(1,3,4)$ data in Figure 3. For the fit, the values of k_1, k_2, k_3, and k_4 previously determined from the PIP and PIP_2 data collected in the presence of GTPγS were used (see Table I). Thus, the only unknown constant in eq C1 is the sum $k_6 + k_9$, and the only unknown constants in eq C2 are k_6' and k_9. The best fits for both sets of data were obtained with the values $k_6 = 0.11$ min^{-1}, $k_6' = 0.18$ min^{-1}, and $k_9 = 0.34$ min^{-1}. Notice that the rate constant for IP_2 production, k_6, determined in Table I by using the simpler model, which ignored the conversion of $IP_3(1,4,5)$ to $IP_3(1,3,4)$ ($k_6 = 0.14$ min^{-1} in the presence of GTPγS), is between the values of IP_2 production from the two isomers of IP_3 (k_6 and k_6').

Registry No. GTP, 86-01-1; GTPγS, 37589-80-3; Ins-1,4,5-P_3, 85166-31-0; Ins-1,3,4-P_3, 93133-76-7; IP_2, 47055-78-7; IP_1, 15421-51-9; phospholipase C, 9001-86-9; PI kinase, 37205-54-2; PIP kinase, 9032-61-5.

References

Berridge, M. J. (1983) *Biochem. J. 212*, 849–858.

Berridge, M. J. (1984) *Biochem. J. 220*, 345–360.

Berridge, M. J., & Irvine, R. F. (1984) *Nature (London) 312*, 315–321.

Berridge, M. J., Dawson, R. M. C., Downes, C. P., Heslop, J. P., & Irvine, R. F. (1983) *Biochem. J. 212*, 473–482.

Bishop, J. M. (1985) *Cell (Cambridge, Mass.) 42*, 23–38.

Cantau, G., Keppens, S., DeWulf, H. D., & Jard, S. (1980) *J. Recept. Res. 1*, 137–168.

Chahwala, S. B., & Cantley, L. (1986) *Biochem. J.* (submitted for publication).

Chu, S. W., Hoban, C. J., Owen, A. J., & Geyer, R. P. (1985) *J. Cell. Physiol. 124*, 391–396.

Cockcroft, S., & Gomperts, B. D. (1985) *Nature (London) 314*, 534–536.

Connolly, T. M., Bross, T. E., & Majerus, P. W. (1985) *J. Biol. Chem. 260*, 7868–7874.

Creba, J. A., Downes, C. P., Hawkins, P. T., Brewster, G., Michell, R. H., & Kirk, C. J. (1983) *Biochem. J. 212*, 733–747.

Della Bianca, V., De Togni, P., Grzeskowiak, M., Vicentini, L. M., & Di Virgilio, F. (1986) *Biochim. Biophys. Acta 886*, 441–447.

Diringer, H., & Friis, R. R. (1977) *Cancer Res. 37*, 2979–2984.

Dixon, J. F., & Hokin, L. E. (1985) *J. Biol. Chem. 260*, 16068–16071.

Downes, C. P., & Wusteman, M. M. (1983) *Biochem. J. 216*, 633–640.

Fleischman, L. F., Chahwala, S. B., & Cantley, L. C. (1986) *Science (Washington, D.C.) 231*, 407–410.

Gilman, A. G. (1983) *J. Clin. Invest. 73*, 1–4.

Gomperts, B. D. (1983) *Nature (London) 306*, 64–66.

Haslam, R. J., & Davidson, M. M. L. (1984) *FEBS Lett. 174*, 90–95.

Hawkins, P. T., Stevens, L., & Downes, C. P. (1986) *Biochem. J. 238*, 501–506.

Heslop, J. P., Irvine, R. F., Tashjian, A., & Berridge, M. J. (1985) *J. Exp. Biol. 119*, 395–401.

Hokin, M. R., & Hokin, L. E. (1953) *J. Biol. Chem. 203*, 967–977.

Irvine, R. F., Letcher, A. J., Heslop, J. P., & Berridge, M. J. (1986) *Nature (London) 320*, 631–634.

Kaplan, D., Whitman, M., Schaffhausen, B., Raptis, L., Garcea, R. L., Pallas, D., Roberts, T. M., & Cantley, L. (1986) *Proc. Natl. Acad. Sci. U.S.A. 83*, 3624–3628.

Litosch, I., & Fain, J. N. (1985) *J. Biol. Chem. 260*, 16052–16055.

Lucas, D. O., Bajjalieh, S. M., Kowalchyk, J. A., & Martin, T. F. J. (1985) *Biochem. Biophys. Res. Commun. 132*, 721–728.

Macara, I. G. (1985) *Am. J. Physiol. 248*, C3–C11.

Macara, I. G., Marinetti, G. V., & Balduzzi, P. C. (1984) *Proc. Natl. Acad. Sci. U.S.A. 81*, 2728–2732.

Majerus, P. W., Wilson, D. B., & Connolly, T. M. (1985) *Trends Biochem. Sci. (Pers. Ed.) 10*, 168–171.

Masters, S. B., Martin, M. W., Harden, T. K., & Brown, J. H. (1985) *Biochem. J. 227*, 933–937.

Mastro, A. M., & Smith, M. C. (1983) *J. Cell. Physiol. 116*, 51–56.

Moreno, F. J., Mills, I., Garcia-Sainz, J. A., & Fain, J. N. (1983) *J. Biol. Chem. 258*, 10938–10943.

Nakamura, T., & Ui, M. (1985) *J. Biol. Chem. 260*, 3584–3593.

Nishizuka, Y. (1984) *Nature (London) 308*, 693–698.

Okajima, F., & Ui, M. (1984) *J. Biol. Chem. 259*, 13863–13871.

Rooijen, L. A., Rossowska, M., & Bazan, N. G. (1985) *Biochem. Biophys. Res. Commun. 126*, 150–155.

Schulz, J., Ling, L., & Cantley (1986) *J. Cell. Biochem. 10 (Suppl. 10C)*, L312.

Streb, H., Irvine, R. F., Berridge, M. J., & Schulz, I. (1983) *Nature (London) 306*, 67–69.

Sugimoto, Y., Whitman, M., Cantley, L., & Erikson, R. L. (1984) *Proc. Natl. Acad. Sci. U.S.A. 81*, 2117–2121.

Taylor, M. V., Metcalf, J. C., Hesketh, T. R., Smith, G. A., & Moore, J. P. (1984) *Nature (London) 312*, 463–466.

Whitman, M., Kaplan, D., Schaffhausen, B., Cantley, L., & Roberts, T. (1985) *Nature (London) 315*, 239–242.

Whitman, M., Fleischman, L., Chahwala, S., Cantley, L., & Rosoff, P. (1986a) *Recept. Biochem. Methodol. 7*, 197–217.

Whitman, M., Kaplan, D., Schaffhausen, B., Roberts, T., & Cantley, L. (1986b) *J. Biol. Chem.* (submitted for publication).

Wilson, D. B., Bross, T. B., Hofmann, S. L., & Majerus, P. W. (1984) *J. Biol. Chem. 259*, 11718–11724.

Wilson, D. B., Neufeld, E. J., & Majerus, P. W. (1985) *J. Biol. Chem. 260*, 1046–1051.